Available online at www.sciencedirect.com
SCIENCE DIRECT®
Journal of Magnetic Resonance 167 (2004) 322–327
JMR Journal of Magnetic Resonance
www.elsevier.com/locate/jmr

Magnetic resonance microscopy of biofilm structure and impact on transport in a capillary bioreactor

Joseph D. Seymour,* Sarah L. Codd, Erica L. Gjersing, and Philip S. Stewart

Department of Chemical and Biological Engineering and Center for Biofilm Engineering, Montana State University, Bozeman, MT, USA

Received 24 November 2003; revised 20 January 2004

Abstract

Microorganisms that colonize surfaces, biofilms, are of significant importance due to their role in medical infections, subsurface contaminant remediation, and industrial processing. Spatially resolved data on the distribution of biomass within a capillary bioreactor, the heterogeneity of the biofilm itself and the impact on transport dynamics for a *Staphylococcus epidermidis* biofilm in the natural growth state are presented. The data demonstrate the ability of magnetic resonance microscopy to study spatially resolved processes in bacterial biofilms, thus providing a basis for future studies of spatially resolved metabolism and in vivo clinical detection.

Keywords: Biofilms; MRI; NMR; Velocity; Propagator

1. Introduction

Biofilms are microorganisms that colonize surfaces. They are of importance in medicine as infections, in bioreactor operation for pharmaceutical and food processing and in environmental bioremediation. Of primary importance are the myriad biomedical applications, as biofilms are the plaque on teeth, the infection on catheters and prosthetic implants and bacterial infections in lungs [1]. Biofilms play a significant role in the resistance of bacteria to antibiotic treatment, proffering resistance to antibiotic concentrations order of magnitudes larger than for suspended cells [2]. This paper presents magnetic resonance microscopy (MRM) measurements of the structure and transport impact of *Staphylococcus epidermidis* biofilms in 1 mm capillary bioreactors. The importance of the results lies in establishing magnetic resonance (MR) methods to study the relation between structure and function in individual naturally occurring biofilms and to establish the basis for future spectroscopic imaging of function. Such studies serve to increase basic understanding of complex multi-phase biological systems and have the potential to enhance clinical diagnostics of biofilm infection by MR.

A key feature of biofilms is the extracellular polymeric substance (EPS) composed of polysaccharides and other biopolymers that surround the bacterial cells in a hydrogel matrix. There is limited knowledge about the mechanics of and diffusion within these viscoelastic biopolymeric gels and hence the effectiveness of agents to penetrate from the bulk fluid to the innermost cells. MR has been applied to image biofilms in their natural growth state in porous media using relaxation time [3,4] and diffusion weighting [5], and in thick, 5–10 mm, microbial mats which occur in oceans and lakes [6]. Other MR studies have used biofilms removed from their natural growth state to concentrate them in order to measure diffusion and to study spectroscopic properties of the hydrogel matrix [7–9]. The only prior applications to a single biofilm in a reactor are the work of Altobelli and coworkers [10] and Manz et al. [11] which imaged the velocity distribution over a single biofilm. The data presented here are unique in that the structure and impact on transport of an individual, 100–300 μm thick biofilm is spatially resolved.

* Corresponding author. Fax: 1-406-994-5308.
E-mail address: jseymour@coe.montana.edu (J.D. Seymour).

1090-7807/$ - see front matter © 2004 Elsevier Inc. All rights reserved.
doi:10.1016/j.jmr.2004.01.009

2. Background and theory

2.1. MR microscopy

MRM methods using relaxation time and diffusion weighting are well established [12]. Structural images of individual biofilms were obtained using a spatially resolved multi-echo CPMG method to generate T_2 maps. This method provides bulk resolution of the biofilm due to restricted mobility of water within the hydrogel matrix and microbe cells. A significant issue in the applicability of MR methods to study structure function relationships in biofilms is the ability to spatially resolve cell clusters within the biofilms in order to measure metabolic activity. Protons within the cell clusters exhibit mobility restricted relative to the EPS hydrogel matrix due to intercellular water, cell membrane water, and intracellular water.

2.2. Biofilms

Techniques currently applied to the study of transport in biofilms are limited in their ability to non-invasively characterize three dimensional structure and convective and diffusive elements of the transport process. Diffusion measuring techniques such as microinjection and confocal microscopy [13], fluorescence recovery after photobleaching (FRAP) [14] and half-cell diffusion studies, where biofilm is grown on a membrane, provide data for the diffusion of different tracer molecules through the biofilm [14–16]. Research on transport in these systems is complicated by the spatial heterogeneity of the biofilm which can cause inaccurate readings in methods such as membrane half-cell studies that monitor the total transport through the membrane and biofilm [14]. Studies of the impact of convection on transport in biofilms have applied confocal microscopy and microelectrode measurements to determine an empirical mass transfer coefficient [17]. However, these techniques cannot provide the quantitative velocity distributions available using MRM. Characterization of the material response, or rheology, of biofilms is also important for predictive modeling of transport due to coupling of momentum and mass conservation and recent characterization by optical measurements of biofilm deformation and tracer motion indicate the viscoelastic nature of biofilms [18].

Application of MR methods to study biofilms is becoming more prevalent. Many applications have focused on the presence of biofilms in porous media due to the importance of these applications in bioremediation and biofiltration [3–5,19]. Studies of the diffusive behavior of biofilms include studies of the diffusion of the water within the biofilm [7] and the polymer molecules themselves [8]. ^{13}C spectroscopy has been applied to determine the integral chemical composition of the extracellular polymeric substance and behavior of the gel as a function of environmental conditions such as electrolyte concentration [9,20]. A primary limitation of most MR studies to date, other than those of biofilms grown in porous media [3,5], is the fact that the biofilms are transferred from their natural growth state on a surface and concentrated for study in the NMR system [7–9,20]. MR studies of single biofilms growing on bioreactors, a state most relevant to biomedical applications, have been limited and either did not image biofilm structure or used a negative contrast agent such as uptake of copper sulfate [10,11]. Bryers and Drummond [14] point out the hydrated gel nature of biofilms and the MR work of Mayer et al. [9,20] verifies the gel structure through identification of proteins, polysaccharides, and nucleic acids in the EPS and comparison of physical response with model gel systems. The polymer gel nature of the EPS is a significant component of reduced nutrient and antimicrobial mass transport in biofilms [14].

2.3. Transport phenomena

Flow in systems of small spatial dimension is typically of negligible inertia, the low Reynolds number, $Re = \langle v_z \rangle l/v$ regime. Re provides a measure of convective to inertial forces, where $\langle v_z \rangle$ is the average velocity, l a typical length scale, and v the fluid kinematic viscosity. In 1976, G.K. Batchelor coined the term microhydrodynamics in reference to flow fields with length scales between 10 nm and 100 μm in which multiple physical processes impact transport, the domain of physicochemical hydrodynamics [21]. This is the regime of interest in biofilm transport due to the biofilm thickness, of the order of magnitude of 100 μm, which impacts boundary layer transport of nutrients, antimicrobial agents, and cells from a free stream to the biofilm impacted surface and the influence of chemical gradients within the EPS matrix. A key feature of low Re hydrodynamics is the limitation of mixing to diffusion across the laminar streamlines of the flow, i.e., hydrodynamic dispersion. Low Re flows in straight smooth walled bioreactors do not exhibit secondary flows, i.e., velocity components in the non-axial direction are identically zero, $v_x, v_y = 0$. Spatial or temporal perturbations that induce secondary flows radically alter the mixing and hence transport of nutrients or biocides in such systems and generate potentially chaotic fluid flow paths due to the higher degrees of freedom that introduce nonlinearity into the problem [22].

Quantitative measurement of these secondary flows is required to model transport when such perturbations are present. Characterization of systems with chaotic fluid particle motions is often accomplished using probability theory concepts to quantify the statistics of the fluid dynamics through quantities such as the probability distribution of velocity [23].

3. Experimental

3.1. Biofilm growth and bacterial strains

The microbial strain *S. epidermidis* was chosen for this research due to the prevalence of this strain in medical implant infections. These studies examined *S. epidermidis* biofilms after 48 h of growth in order to have optimal quantities of biofilm present to test the capabilities of the MRM techniques. The *S. epidermidis* biofilms were grown in 1 mm square glass capillaries connected to nutrient feed and waste carboys with silicone tubing. Square capillaries are used in order to facilitate analysis of biofilms with laser confocal microscopy and MRM. A flow break was used upstream of the biofilm to insure a steady feed rate and the glass capillary was placed in a metal flow cell holder to prevent breakage. After the reactor system was set up, it was inoculated from downstream with a culture of suspended *S. epidermidis* bacteria for 4 h. Gravity driven flow was then started at a flow rate of 0.028 ml/s, for an average velocity of 28 mm/s and $Re = 45$, which fed 1/10th strength Tryptic Soy Broth (TSB) to the biofilm for 48 h. The bacteria and growth media were incubated at 37 °C during all stages of the growth period since *S. epidermidis* grows most prolifically at human body temperature. After the 48 h growth period, the biofilm was placed inside the NMR magnet.

3.2. MRM experiments

MRM experiments were performed on a Bruker Avance DRX spectrometer networked to a 250 MHz standard bore superconducting magnet. A Bruker Micro5 microimaging probe and gradient amplifiers adapted the spectrometer to allow microimaging using gradients coils capable of 2 T/m. The location of the biofilm is mapped in three dimensions and the fluid dynamics both of the bulk fluid and within the structure are measured using the ^{1}H signal from water. A standard medical contrast agent which is chelated to avoid uptake by the cells (Magnevist, Berlex Laboratories) was added at a concentration of 0.6 ml/L of water to allow faster repetition times.

T_2 maps were obtained in the absence of flow using a slice selection 2-D multi-spin echo imaging sequence with a recovery time, TR = 500 ms, and 8 echo times (TE = 10, 20, ..., 80 ms); Slice thickness was 0.3 mm, FOV of 2.5×20 mm, and image resolution 19.5×156 μm. Total imaging time to generate the data to calculate the T_2 maps was 8.5 min. The velocity maps were obtained using the Bruker DWI_SE sequence, which is a flow spin-warp imaging sequence flow sensitized by a bipolar gradient pair (Imaging parameters: TR = 2000 ms, TE = 20 ms, slice thickness = 0.3 mm, FOV = 2.5×20 mm, and resolution = 39×156 μm) with two displacement encoding gradients ($g = 0$, 100 mT/m, $\delta = 1$ ms, and $\Delta = 4$ ms). The velocity maps were acquired in 17 min. The propagators were obtained using a pulsed gradient spin echo (PGSE) method, with a gradient pulse separation time of $\Delta = 15$ ms, a gradient pulse duration time $\delta = 2$ ms and 128 gradient value steps from −1000 to 1000 mT/m in order to fully sample q-space [24]. Volumetric flow rates of 0.01 ml/s corresponding to an average velocity of 10 mm/s, and $Re = 16$ in the clean bioreactor, were studied.

4. Results and discussion

The T_2 maps shown in Fig. 1 clearly display the structure of the biofilm with dark colors corresponding to high mobility, high T_2 free water proton signal and light colors representing low mobility, low T_2 restricted water proton signal. Since *S. epidermidis* are non-motile bacteria, the biofilm concentration is greatest on the capillary reactor wall which was at the bottom during innoculation, Fig. 1A, due to settling of the microbes on that surface. Fig. 1B shows a slice through the capillary center. The biofilm is composed of clusters of biomass in which channels and hollow central regions are visible, demonstrating the ability of MRM to characterize the spatial heterogeneity of the biofilm within the reactor. In addition the heterogeneous nature of the biofilm itself is clearly evident in Fig. 1 from the regions of water with restricted mobility, lighter colors of lower T_2, dispersed within the orange intensity biomass. These regions of light color are lower mobility regions that correspond to either cell clusters within the EPS matrix or regions of gel matrix with higher polymer concentration. Studies in which MR sensitive molecular tags attach to cells have the potential to identify cell clusters directly. The ability to spatially resolve the biofilm at the resolution demonstrated here provides the opportunity to extend bulk NMR spectroscopy [9,20] and spectrally resolved diffusion [8] measurements to natural state biofilms. This advance would provide a means for spatially resolved metabolic function studies to be coupled to molecular dynamics, as well as provide a basis for in vivo clinical detection of biofilms.

Many of the features present in the images in Fig. 1 are obtainable by other techniques such as confocal microscopy, which can provide higher spatial resolution (~1 μm) than MR but does not provide depth resolved information, chemical spectra or molecular dynamics. Fig. 2 shows MR velocity maps of the axial velocity, v_z, as a function of the (x, z) coordinates and (x, y) coordinates for low Re flow of water in a clean 1 mm bioreactor. The spatial velocity distribution is maximal at the tube center with regions of slow flow in the corners of the square duct in exact agreement with solution of the momentum conservation equations for the system

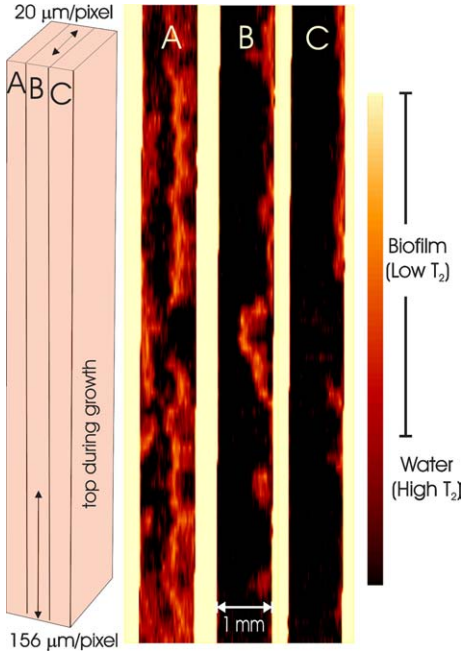

Fig. 1. Biofilm Structure: The T_2 maps on the left show three slices through a mature *S. epidermidis* biofilm, grown in a 1 mm square bioreactor for 48 h. Slice thickness is 300 μm. Pixel resolution is 19.5 μm across the width and 156 μm along the length. (A) Bottom slice, (B) middle slice, and (C) top slice relative to gravity during growth.

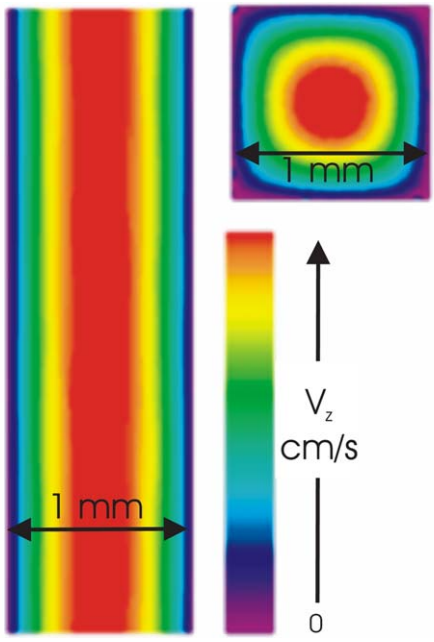

Fig. 2. (A) Experimental velocity maps for water flowing in a clean square capillary at $Re = 16$, note the axial velocity is only a function of the cross section spatial coordinates not the axial coordinate, $v_z = v_z(x, y)$.

generated in MATLAB. The axial velocity is the only component present and is a function only of the cross section coordinates, $v_z = v_z(x, y)$. Velocity maps of the x

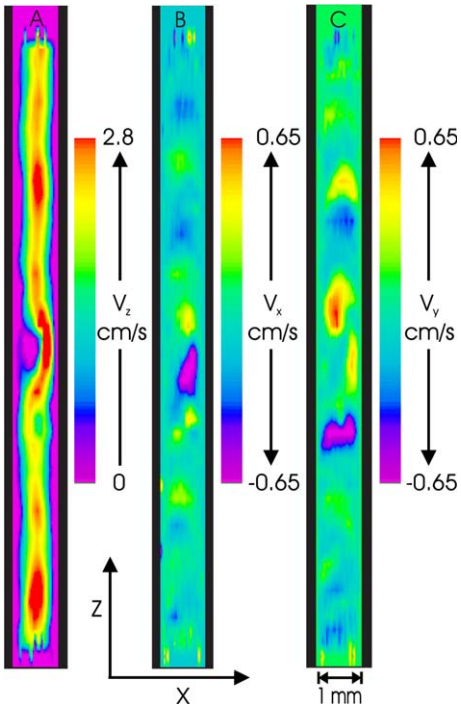

Fig. 3. Velocity maps around mature biofilm structure: The images show the velocities of water flowing upward in the middle slice through a mature *S. epidermidis* biofilm. Slice thickness is 200 μm. Pixel resolution is 39 μm across the width and 156 μm along the length. (A) z-Direction component of the velocity, red indicates where flow is the fastest and purple indicates where there is no flow. (B) x-Direction (left and right) component of the velocity, red indicates where flow is the fastest to the left and purple indicates where flow is the fastest to the right. (C) y-Direction (in and out) component of the velocity. Note the significant secondary flows in the x and y directions not present in a clean bioreactor.

and y velocity components (not shown) exhibit no secondary flows for the clean capillary as is expected. The only mechanism for mixing in such a flow is molecular diffusion across streamlines causing Taylor dispersion [25].

Velocity images taken for a slice in the center of the bioreactor with biofilm present, Fig. 3, show several important aspects of variation in transport due to the perturbation effect of the biofilm. Most dominant is the initiation of secondary flows. The mechanism for initiation of the secondary flows is the irregular spatial distribution of the viscoelastic biofilm as a boundary condition on the flowing fluid. A large biofilm nodule as is seen in the T_2 map of Fig. 1B in the bioreactor center is similar in nature to the nodule in Fig. 3A on the left wall which shows no velocity within the biofilm but a strong perturbation on the flow field. An interesting feature for future study of the secondary flow is the resemblance to Taylor vortices and Rayleigh–Benard convection type hydrodynamic instabilities, which tend to scale with flow channel size, despite the different mechanisms for initiation of secondary flow in the

bioreactor. The presence of the biofilm and the induced secondary flows cause axial velocity variations as a function of axial position as well. The importance of secondary flows is the significant variation in mixing mechanism they represent, since all three components of the velocity vector, **v**, are now present and each depends on all three spatial dimensions, $\mathbf{v} = (v_x(x,y,z), v_y(x,y,z), v_z(x,y,z))$. The conservation of momentum equations result in three coupled partial differential equations, the solution to which is potentially unstable in a hydrodynamics context and requires numerical methods. An important feature of the velocity data is that inside the biofilm biomass, the velocity is zero within the phase resolution of the MRM velocity data. This indicates the low permeability of the EPS hydrogel material.

A strength of MR methods for the characterization of complex flows is the ability to both spatially resolve velocity and statistically characterize the dynamics by measurement of the propagator using PGSE. The propagator of the axial displacements, $Z = z(\Delta) - z(0)$, for short displacement observation times Δ, is the probability distribution of the velocity $P(v_z) = P(Z,\Delta)$ since for short times $v_z = Z/\Delta$ [24]. Fig. 4 shows measured velocity probability distributions, i.e., short Δ propagators, for the clean bioreactor (solid gray line) and the biofilm impacted bioreactor (solid black line).

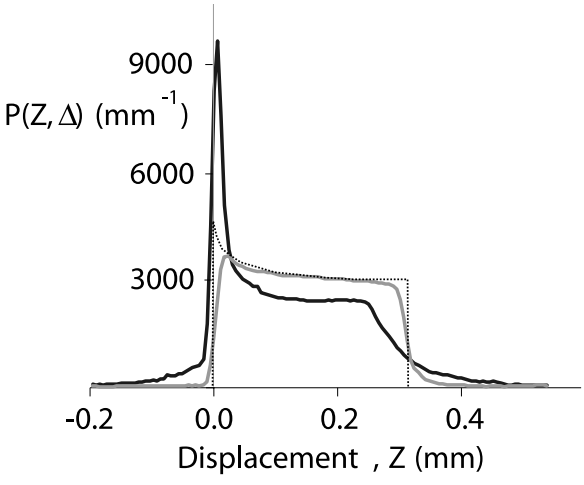

Fig. 4. Experimentally measured propagators for flow in the clean square capillary (solid gray line) and for flow in a biofilm fouled square capillary (solid black line), for an observation time Δ of 15 ms. The theoretical propagator (dashed black line) calculated from the MATLAB generated velocity distribution for the clean capillary is also shown. Agreement between the two is excellent when one accounts for the fact the experimental propagator (solid gray line) is the theoretical propagator (dashed black line) convolved with a Gaussian point spread function proportional to the dispersion at each velocity over the observation time Δ of 15 ms. In the propagator for flow around the biofilm structure (solid black line) note the appearance of a high velocity tail showing the higher probability of large displacements. The slow flow peak near zero displacement results from the protons trapped within the EPS gel matrix where the primary transport mechanism is diffusive.

Also shown in Fig. 4 is a histogram of velocity from the MATLAB solution, or theoretical propagator (dotted black line) for flow in a clean square capillary. The measured and theoretical probability distribution of velocity for the clean reactor demonstrate excellent agreement, indicating a near box function, as expected for circular pipe flow [24,25] with a peak at low velocities corresponding to the slow flows in the corners of the square bioreactor. The clean reactor experimental propagator is broadened due to molecular diffusion during the observation time Δ which is not present in the theoretical propagator, i.e., the velocity distribution is convolved with a Gaussian point spread function proportional to the dispersion at each velocity over the observation time of 15 ms. Comparison of the clean (solid gray line) and biofilm impacted (solid black line) propagators indicates the significant change in dynamics caused by biofilm growth. The biofilm propagator (solid black line) exhibits a large peak centered at zero displacement due to the water restricted within the EPS gel matrix. Also evident is an increase in probability for negative displacements larger than the broadening due to diffusion. This is reasonable given the viscoelastic nature of the biofilm which can generate oscillations at the biofilm fluid interface [18] which must induce negative displacements. The most important feature is the large displacement tail of the distribution that indicates significant probability of large displacements that is absent in the clean bioreactor. The higher probability of large displacements is typical of complex flows which exhibit chaotic fluid motion and are key to the statistical characterization of mixing by quantifying less probable large events.

5. Conclusions

This paper demonstrates that high resolution MRM can be applied to study individual biofilms in their natural state and can directly measure the heterogeneity within the biomass. As such, it extends current applications of MR from bulk characterization of biofilms in condensed non-native states and negative contrast imaging to include internal structure characterization. It is also demonstrated that biofilms induce a transition in bioreactor scale dynamics which alter the mechanisms of transport for nutrients and biocides. The complex dynamics are characterized by spin populations exhibiting highly restricted motion within the EPS gel matrix and large displacements due to fast flow paths generated by the heterogeneous distribution of biofilm within the reactor. The data presented provides the basis for pursuit of spatially and spectrally resolved molecular dynamics to probe the spatial distribution of biofilm metabolism thereby elucidating structure–function relationships in these important systems.

Acknowledgments

S.L.C. and J.D.S. acknowledge funding from the MSU Office of the VP of Research, DOE EMSP Grant DE-FG02-03ER63576, and acknowledgement is made to the Donors of the American Chemical Society Petroleum Research Fund for partial support of this research. E.L.G. is funded by an award from the W.M. Keck Foundation. Acknowledgment is made to Dieter Gross of Bruker for assistance with the Micro5 probe and Berlex Laboratories for providing us free samples of Magnevist for research purposes.

References

[1] J.W. Costerton, P.S. Stewart, Battling biofilms, Sci. Am. 285 (2001) 1.
[2] P.S. Stewart, J.W. Costerton, Antibiotic resistance of bacteria in biofilms, The Lancet 358 (2001) 135.
[3] B.C. Hoskins, L. Fevang, P.D. Majors, M.M. Sharma, G. Georgiou, Selective imaging of biofilms in porous media by NMR relaxation, J. Magn. Reson. 139 (1999) 67.
[4] K.P. Nott, M. Paterson-Beedle, L.E. Macaskie, L.D. Hall, Visualization of metal deposition in biofilm reactors by three-dimensional magnetic resonance imaging (MRI), Biotechnol. Lett. 23 (2001) 1749.
[5] K. Potter, R.L. Kleinberg, F.J. Brockman, E.W. McFarland, Assay for bacteria in porous media by diffusion-weighted NMR, J. Magn. Res. B 113 (1996) 9.
[6] A. Wieland, D. de Beer, L.R. Damgaard, M. Kuhl, D. van Dusschoten, H. van As, Fine-scale measurement of diffusivity in a microbial mat with nuclear magnetic resonance imaging, Limnol. Oceanogr. 46 (2001) 248.
[7] E.E. Beuling, D. van Dusschoten, P. Lens, J.C. van den Heuvel, H. van as, P.P. Ottengraf, Characterization of the diffusive properties of biofilms using pulsed field gradient-nuclear magnetic resonance, Biotechnol. Bioeng. 60 (1998) 283.
[8] M. Vogt, H.-C. Flemming, W.S. Veeman, Diffusion in *Pseudomonas aeruginosa* biofilms: a pulsed field gradient NMR study, J. Biotechnol. 77 (2000) 137.
[9] C. Mayer, R. Moritz, C. Kirschner, W. Borchard, R. Maibaum, J. Wingender, H.-C. Flemming, The role of intermolecular interactions: studies on model systems for bacterial biofilms, Int. J. Biol. Macromol. 26 (1999) 3.
[10] Z. Lewandowski, P. Stoodley, S.A. Altobelli, E. Fukushima, Hydrodynamics and kinetics in biofilm systems—recent advances and new problems, Water Sci. Technol. 29 (1994) 223.
[11] B. Manz, F. Volke, D. Goll, H. Horn, Measuring local flow velocities and biofilm structure in biofilm systems with magnetic resonance imaging (MRI), Biotechnol. Bioeng. 85 (2003), 10.1002/10782.
[12] P.T. Callaghan, Principles of Nuclear Magnetic Resonance Microscopy, Oxford University Press, New York, 1991.
[13] D. de Beer, P. Stoodley, Z. Lewandowski, Measurement of local diffusion coefficients in biofilms by microinjection and confocal microscopy, Biotechnol. Bioeng. 53 (1997) 151.
[14] J.D. Bryers, F. Drummond, Local macromolecule diffusion coefficients in structurally non-uniform bacterial biofilms using fluorescence recovery after photobleaching (FRAP), Biotechnol. Bioeng. 60 (1998) 462.
[15] C. Nicoletta, P. Pavasant, A.G. Livingston, Substrate counterdiffusion and reaction in membrane-attached biofilms: mathematical analysis of rate limiting mechanisms, Chem. Eng. Sci. 55 (2000) 1385.
[16] P.S. Stewart, A review of experimental measurements of effective diffusion permeabilities and effective diffusion coefficients in biofilms, Biotechnol. Bioeng. 59 (1998) 261.
[17] P. Stoodley, S. Yang, H.M. Lappin-Scott, Z. Lewandowski, Relationship between mass transfer coefficient and liquid flow velocity in heterogeneous biofilms using microelectrodes and confocal microscopy, Biotechnol. Bioeng. 56 (1997) 681.
[18] P. Stoodley, Z. Lewandowski, J.D. Boyle, H.M. Lappin-Scott, Structural deformation of bacterial biofilms caused by short-term fluctuations in fluid shear: an in situ investigation of biofilm rheology, Biotechnol. Bioeng. 65 (1999) 83.
[19] H. van As, P. Lens, Use of 1H NMR to study transport processes in porous biosystems, J. Ind. Microbiol. Biotechnol. 26 (2001) 43.
[20] C. Mayer, D. Lattner, N. Schurks, ^{13}C nuclear magnetic resonance studies on selectively labeled bacterial biofilms, J. Ind. Microbiol. Biotechnol. 26 (2001) 62.
[21] G.K. Batchelor, in: W.T. Koiter (Ed.), Theoretical and Applied Mechanics, North-Holland, Amsterdam, 1976, p. 33.
[22] J.M. Ottino, The Kinematics of Mixing: Stretching, Chaos and Transport, Cambridge University Press, Cambridge, 1989.
[23] A.J. Lichtenberg, M.A. Lieberman, Regular and Chaotic Dynamics, Springer-Verlag, New York, 1992.
[24] P.T. Callaghan, S.L. Codd, J.D. Seymour, Spatial coherence phenomena arising from translational spin motion in gradient spin echo experiments, Concept. Magnetic Res. 11 (1999) 181.
[25] S.L. Codd, B. Manz, J.D. Seymour, P.T. Callaghan, Taylor dispersion and molecular displacements in poiseuille flow, Phys. Rev. E 60 (1999) R3491.